



## Measurement of Gradient Magnetic Field Temporal Characteristics ✓

Bartušek Karel, Jílek Blahoslav  
Czech Academy of Sciences, Institute of Scientific Instruments  
Kralovopolska 147, 61264 Brno, Czech Republic

We describe a technique of measuring the time dependence and field distortions of magnetic fields due to eddy currents (EC) produced by time-dependent magnetic field gradients. The EC measuring technique makes use of a large volume sample and selective rf excitation pulses and free induction decay (FID) (or a spin or gradient echo) to measure the out-of-phase component of the FID, which is proportional to  $\gamma\Delta B$ , i.e. the amount the signal is off resonance. The measuring technique is sensitive, easy to implement and interpret, and used for determining pre-emphasis compensation parameters.

### 1. Introduction

A number of NMR experiments use pulsed field gradients and are adversely affected by any departure of the gradient from the desired temporal field. Examples are found in the field of pulsed-gradient spin-echo NMR (1), during slice selection in NMR imaging (2), and in localized spectroscopy. All these techniques require gradients with very short switching times. However, particularly for superconducting magnets, the pulsed gradients induce eddy currents in conducting structures of the magnet which generate undesired time-variable magnetic fields in the volume of interest. Many familiar different techniques have been employed to compensate for, or to minimize, such EC distortions of magnetic field gradient pulses. For these methods, the accuracy of compensation for the influence of EC depends on the perfection of measurement of the time characteristics of the decay gradient magnetic fields. The use of the NMR signal as a monitor of the time-dependent magnetic field gradient (3-8) has certain disadvantages. One problem is that the gradient quickly dephases the signal with the gradient off.

Two techniques (7) and (8) helped us solve this problem. A small size sample was positioned off the centre of the gradient system and was excited by a series of RF pulses. Many FIDs were detected and time characteristics of the gradient pulses were determined from the frequency shift or instantaneous frequency of the FIDs. Main problems of these methods are inaccuracies in placing the sample at right positions, and using a special sample or phantom, and a small S/N ratio in the MULTIFID technique (8) (RF pulses  $\beta = 5^\circ$ ), and a lower sensitivity of measurement (7) (broad linewidth of the short  $T_2$  sample).

### 2. Method

We think that it is suitable to use for the measurement of time characteristics of gradient magnetic fields either a large-size sample or a large-size phantom that will be influenced by inhomogeneities in a great volume and will, at the same time, give a maximum NMR signal. The advantage of this approach is the simplicity and the high speed of the measuring experiment on the NMR tomograph and a high attainable accuracy of measurement. Therefore, a spherical phantom of 15 mm in diameter (i.e. the maximum size of the working space) filled with water and positioned in the electric centre of the gradient system was used. The nuclei excited in the thin layer off the electric centre will give in the gradient magnetic field a signal the instantaneous frequency of which is proportional to the change in the magnetic field. The pulse sequence for measurement of time characteristics of

gradients is shown in Fig. 1. The gradient under measurement is switched on 2 s before the rf pulse, in order to stabilize the eddy currents. To determine the gradient amplitude, the FID signal is recorded for a period of 1 ms within the gradient, and the detection of the NMR signal after switching off the gradient lasts more than 200 ms.

The excited layer can possibly be delimited mechanically, using a sample of suitable shape. The inhomogeneity of the basic magnetic field causes however a faster dephasing of the FID signal and its shortening. As a result, the time of measurement gets shorter. Therefore, the layer is excited by the 12 ms rf rectangular pulse during gradient field applied, see Fig. 2.

For the sample position  $z_0$ , the spatial distribution of the measured gradient magnetic field  $G_z$  can be described by the relations

$$B_z(z_0, t) = B_0(t) + G_z(t) z_0$$

The position  $z_0$  is defined by the excitation offset  $\omega_B$ . The FID signal for a cubic sample can be described by the equation

$$M_T = M_0 \exp \left[ i \left( \omega_B t - \omega_D t - \Phi(t) \right) - \frac{t}{T_2^*} \right] \frac{\sin(\Delta \omega t)}{\Delta \omega t}$$

where

$$\Phi(t) = \gamma \int_0^t B_z(z_0, t) dt$$

$\omega_B$  is excitation frequency

$\omega_D$  is reference detection frequency

$T_2^*$  is relaxation time of cores

$\Delta \omega$  is frequency width of cubic layer

On deriving the time characteristic of the phase of the complex FID  $\Phi(t)$ , its instantaneous frequency  $f(t)$ , is proportional to the time characteristic of the magnetic field  $B_z(z_0, t)$

$$f(t) = \frac{d}{dt} [\Phi(t)] = \gamma B_z(z_0, t)$$

The signal amplitude will decrease with decreasing frequency width, but the FID dephasing time (time of measurement) will increase. The magnitude of noise is proportional to the receiver band width and does not depend on the way of exciting. To decrease the noise, the transmitting offset  $\omega_B$  can be changed to  $\omega_D$  during the detection and then the filter bandwidth can be halved. The parameters are chosen so that they are optimum for the maximum S/N ratio during the whole time of measurement, i.e. a low offset  $\omega_B$ , a small amplitude of the gradient and a small frequency bandwidth of the excited layer which is limited by the maximum length of the selective pulse and by the relaxation of cores  $T_2^*$ .

The data were processed in several steps. The first was the determination of the instantaneous phase of the complex FID signal. The second step was the derivation of the phase fig.3b and adaptive moving average filtration of the instantaneous frequency fig.3c, because the phase noise is non-linearly proportional to the S/N ratio drop of the FID

amplitude. The third step was the implementation the Nelder-Mead simplex algorithm for nonlinear fitting and for determination of the pre-emphasis constants.

### 3. Experimental results

The measurement was carried out using a home-built 200 MHz spectrometer with a probe allowing microhomography. The maximum diameter of the sample used was 20 mm. The spectrometer is equipped with the gradient system  $G_x$ ,  $G_y$ ,  $G_z$ ,  $G_{zo}$ . The amplitude of the gradient pulse measured was 3.2 mT/m.

The magnetic field was measured for a time of 1 ms for a full gradient amplitude (fig.1) in order to determine its magnitude and to record the time characteristic close after it had been switched off. The overall time of measurement was 300 ms (fig.3a); it depends on the homogeneity of the basic field which mostly determines the FID signal length. An extension of the time of measurement and an increase in the S/N ratio can be achieved by using a gradient or spin echo. The  $90^\circ$  transmitting pulse excited the nuclei at the frequency  $\omega_E = 400$  Hz from resonance. The detection frequency was  $\omega_D = -400$  Hz, and the bandwidth was limited by the 2 KHz filter and was chosen so that the influence of the properties of the filter used (phase characteristic and step response) on the measurement accuracy and noise level was minimum.

In order to improve the S/R ratio, the signal was accumulated forty times. Figures 4,5,6 and 7 give the time characteristics of the gradient magnetic field  $G_x(t)$ ,  $G_y(t)$ ,  $G_z(t)$ , and  $G_{zo}(t)$  measured after the gradient has been switched off. The summary of the pre-emphasis time and amplitude constants for all measured gradients and for the  $G_x$  gradient, which was measured by the MULTIFID method (8) for the same magnet system, can be seen in table1.

### 4. Conclusion

The described NMR method is based on the measurement of an instantaneous frequency of the FID signal, recorded immediately after switching off the gradient pulse. The method was used for a fast and sufficiently accurate determination of the pre-emphasis time and amplitude constants. The large volume sample, the accurate localization of the measured layer by selective  $90^\circ$  rf pulse and adaptive moving average filtering were used. The determined pre-emphasis constants for the same magnet system measured by different methods are alike, and the pre-emphasis compensation of our magnet by the gradient system with the digital signal processor DSP96000 will be made.

### References

1. E.O.Stejskal and J.E.Tanner, J.Chem.Phys. **42**,288 (1965)
2. A.N.Garroway, R.K.Grannell, and P.Mansfield, J.Phys.C**7**, 456 (1974)
3. M.A.Morich, D.A.Lampman, W.R.Dannels, and F.T.D.Goldie, Trans.Med.Imag. **7**, 247 (1988)
4. J.J.Van Vaals and Bergman, J.Magn.Reson. **90**, 52 (1990)
5. P.Jehenson, M.Westphal, and N.Schuff, J.Magn.Reson. **90**, 264 (1990)
6. E.Yamamoto and H.Kohno, J.Phys.E:Sci.Instrum. **12**, (1986)
7. R.E.Wysong and I.J.Lowe, Magn.Reson.Med. **22**,119 (1993)
8. K.Bartušek and V.Puczok, Meas.Sci.Technol. **4**, 357 (1993)

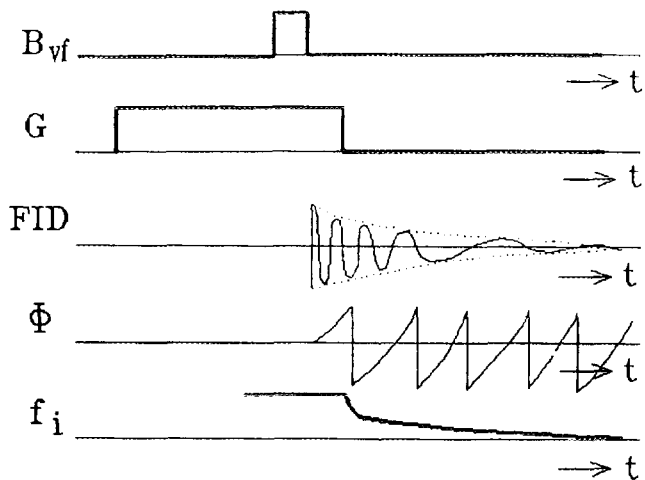


Figure 1. The pulse sequence

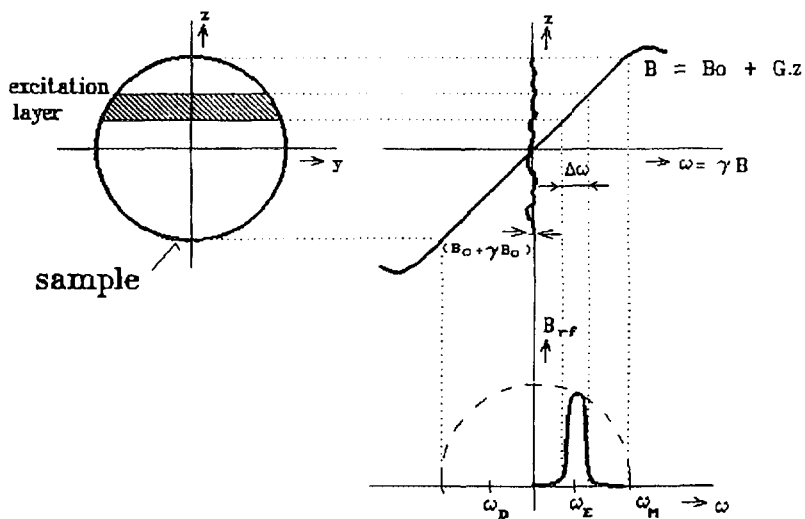


Figure 2. The selective excitation of the large volume sample

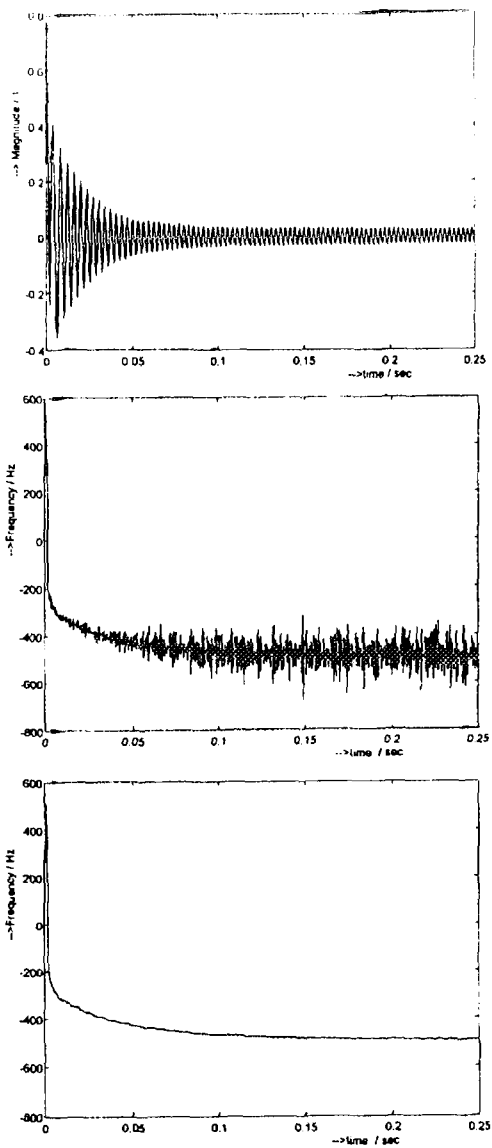


Figure 3. Signal processing:  
 3a) measured FID  
 3b) instantenous frequency without any filtration  
 3c) instantenous frequency with adaptive moving average filtration

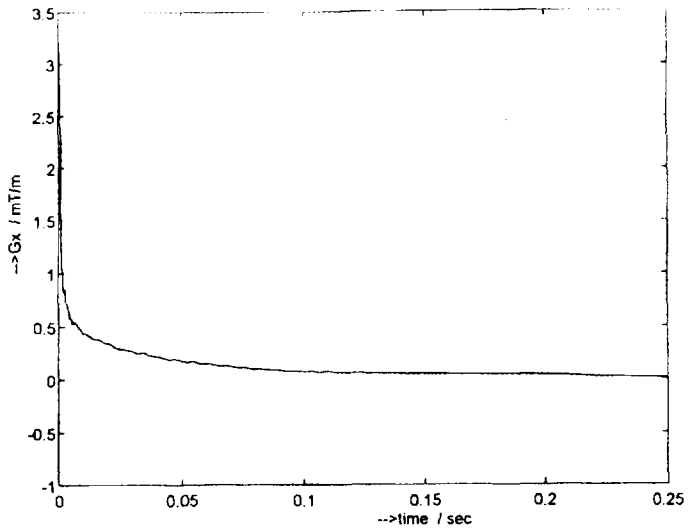


Figure 4. The time characteristic of the  $G_x(t)$  gradient field.

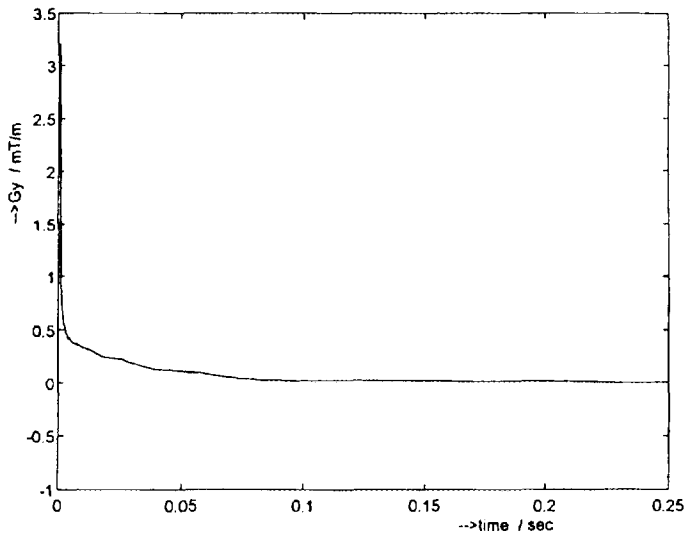


Figure 5. The time characteristic of the  $G_y(t)$  gradient field.

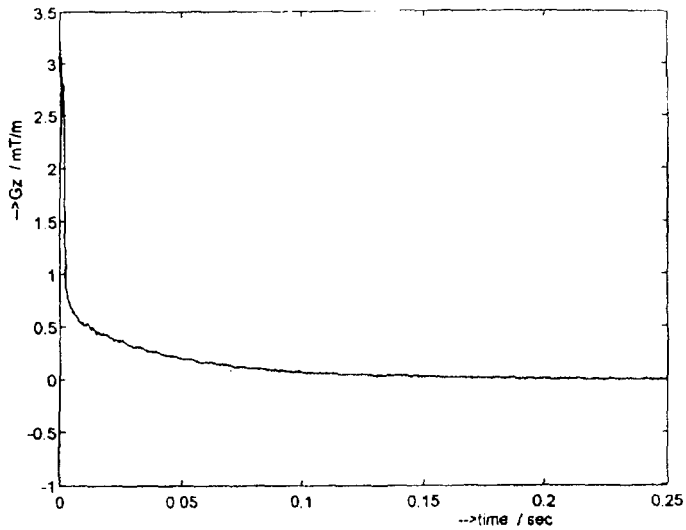


Figure 6. The time characteristic of the  $G_z(t)$  gradient field.

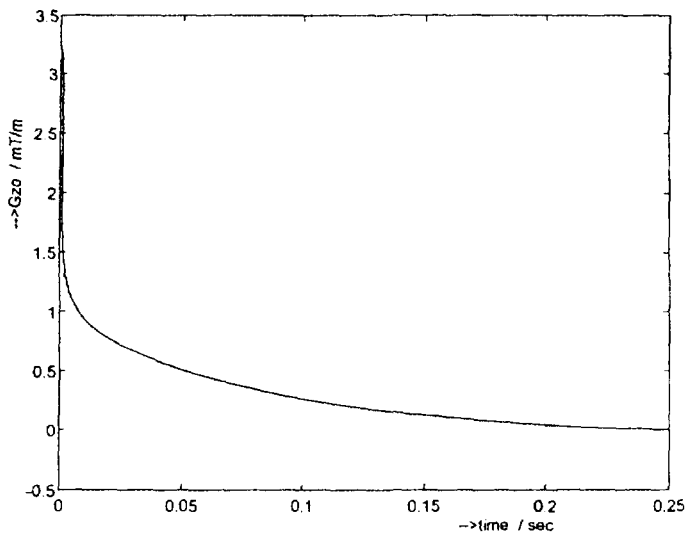


Figure 7. The time characteristic of the  $G_w(t)$  gradient field

Table 1.: The system time and amplitude constants for measured gradients.

gradient mT/m	time constants ms	magnitude %
$G_x$	0.16	78
	3.9	12.3
	54.9	9.7
$G_y$	0.14	70.0
	13.9	16.6
	37.5	13.4
$G_z$	0.28	71.5
	4.19	8.5
	42.14	21.3
$G_{zo}$	0.39	61.3
	3.77	10.4
	66.3	31.4
<b>MULTIFID</b>		
$G_z$	0.07	32.8
	1.78	12.8
	34.8	23.9